Environmental Science & Technology

Article

pubs.acs.org/est

# $TiO_2$-Photocatalytic Reduction of Pentavalent and Trivalent Arsenic: Production of Elemental Arsenic and Arsine

Ivana K. Levy,[†,‡,§] Martín Mizrahi,[∥] Gustavo Ruano,[⊥] Guillermo Zampieri,[⊥,#,‡] Félix G. Requejo,[∥,‡] and Marta I. Litter*[,†,‡,▽]

[†]Gerencia Química, Comisión Nacional de Energía Atómica, Avenida General Paz 1499, 1650 San Martín, Prov. de Buenos Aires, Argentina

[‡]Consejo Nacional de Investigaciones Científicas y Técnicas (CONICET), Av. Rivadavia 1917, 1033 Ciudad Autónoma de Buenos Aires, Argentina

[§]Facultad de Ciencias Exactas y Naturales, Universidad de Buenos Aires, Ciudad Universitaria, Pabellón 2, 1428, Ciudad Autónoma de Buenos Aires, Argentina

[∥]Instituto de Investigaciones Fisicoquímicas Teóricas y Aplicadas (INIFTA-CONICET), Dto. de Química y Dto. de Física, Facultad de Ciencias Exactas, Universidad Nacional de La Plata, Diag. 113 y 64, 1900 La Plata, Argentina

[⊥]Centro Atómico Bariloche, Comisión Nacional de Energía Atómica, Av. Bustillo 9500, 8400 Bariloche, Argentina

[#]Instituto Balseiro, Universidad Nacional de Cuyo, Av. Bustillo 9500, 8400 Bariloche, Argentina

[▽]Instituto de Investigación e Ingeniería Ambiental, Universidad Nacional de General San Martín, Peatonal Belgrano 3563, 1° piso, 1650 San Martín, Provincia de Buenos Aires, Argentina

Supporting Information

**ABSTRACT:** Heterogeneous photocatalytic reduction of As(V) and As(III) at different concentrations over $TiO_2$ under UV light in deoxygenated aqueous suspensions is described. For the first time, As(0) was unambiguously identified together with arsine ($AsH_3$) as reaction products. As(V) reduction requires the presence of an electron donor (methanol in the present case) and takes place through the hydroxymethyl radical formed from methanol oxidation by holes or hydroxyl radicals. On the contrary, As(III) reduction takes place through direct reduction by the $TiO_2$-conduction band electrons. Detailed mechanisms for the photocatalytic processes are proposed. Although reduction to solid As(0) is convenient for purposes of As removal from water as a deposit on $TiO_2$, attention must be paid to formation of $AsH_3$, one of the most toxic forms of As, and strategies for $AsH_3$ treatment should be considered.

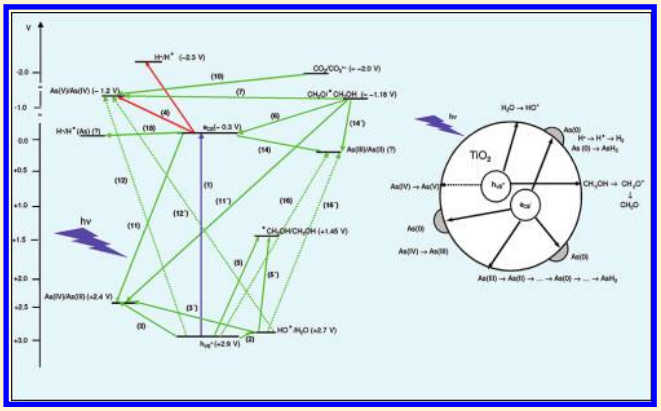

## INTRODUCTION

Toxicity of arsenic (As) is well-known. Ingestion of small amounts for a long period leads to the occurrence of arsenicosis or chronic regional endemic hydroarsenicism ("hidroarsenicismo crónico regional endémico", HACRE, in Spanish), responsible for skin alterations and cancer.[1,2] The World Health Organization recommends 10 $\mu g\ L^{-1}$ as the maximum allowable As concentration in drinking water.[3] Predominant As forms in natural waters are arsenate ($H_2AsO_4^-$ and $HAsO_4^{2-}$) and arsenite (as neutral $As(OH)_3$). Methods for As removal from waters are urgent, but they should take into account that As(III), more toxic and mobile than As(V), is more difficult to remove due to its nonionic form at pH < 9.[1] Conversion to solid As(0) could be an interesting idea for As immobilization.

Heterogeneous photocatalysis with $TiO_2$ (HP) is one of the most studied advanced oxidation processes for water treatment. After irradiation with photons of adequate energy, electrons in the conduction band ($e_{CB}^-$) and holes in the valence band ($h_{VB}^+$) are produced, followed by redox reactions with solution species.[4−6] The commercial P25 form (Evonik) is the most investigated $TiO_2$ photocatalyst.

$$TiO_2 + h\nu \rightarrow e_{CB}^- + h_{VB}^+ \quad (1)$$

Oxidative HP reactions of As(III) to As(V) over $TiO_2$ have been thoroughly studied,[1,2,6−31] and proposed to occur through monoelectronic oxidation to As(IV), easily driven by $HO^\bullet$ produced from water (eqs 2 and eq 3, 3′), or by $h_{VB}^+$ (eq 3),

Received: July 29, 2011
Revised: November 27, 2011
Accepted: January 5, 2012
Published: January 5, 2012

   dx.doi.org/10.1021/es202638c | Environ. Sci. Technol. 2012, 46, 2299−2308

taking into account the redox level of $h_{VB}^+$ generated from P25 (+2.9 V),[32] the value of the reduction potential of the $HO^\bullet$/$H_2O$ couple ($E^0 \approx +2.7$ V)[33] and that of the As(IV)/As(III) couple ($E^0 \approx +2.4$ V).[34] Note that all reduction potentials in this paper are standard values vs NHE.

$$H_2O + h_{VB}^+ \rightarrow HO^\bullet + H^+ \quad (2)$$

$$As(III) + h_{VB}^+\{HO^\bullet + H^+\} \rightarrow As(IV)\{H_2O\} \quad (3, 3')$$

On the contrary, HP reduction of As(V) or As(III) has been scarcely studied,[7,10,14,25] with evidence that As(V) HP reduction might be much slower than As(III) HP oxidation.[8] Actually, reduction of As(V) to As(IV) by $e_{CB}^-$ (eq 4) is not thermodynamically possible ($E^0 \approx -1.2$ V)[34] in relation with the reduction level of P25 $e_{CB}^-$ ($\approx -0.3$ V):[32]

$$As(V) + e_{CB}^- \rightarrow As(IV) \quad (4)$$

However, an indirect reductive mechanism might take place in the presence of sacrificial electron donors like alcohols or carboxylic acids, able to produce strongly reductive radicals. In agreement, negligible As(V) HP removal was observed in the absence of electron donors (anoxic conditions), but removal was actually possible in the presence of different electron donors.[7,29] On the other hand, As(III) reduction was never proposed and, generally, only oxidation to As(V) in solution was evaluated.[10,14] In other HP studies with As(III) in deoxygenated media, with good electron acceptors such as $CCl_4$, POM, bromate, $Cu^{2+}$ or $Ag^+$, the authors did not observe As(III) reduction but, conversely, observed an enhanced As(III) oxidation.[11,14−16,19,22]

An experimental evidence of As(III) reduction, observed by some authors but never taken into account, was the change of color of the white $TiO_2$ suspension to gray, erroneously attributed to the accumulation of trapped electrons in $TiO_2$ particles.[9,13] The only exception was Yang et al.,[7] who proposed As(0) formation; however, the XPS spectrum presented in that paper is only a rapid survey scan without exact resolution of the components.

In this paper, reduction of As(V)/(III) species by $TiO_2$−HP under anoxic conditions is revisited and thoroughly analyzed. As(III) effective reduction in the absence of donors, and clear identification of As(0) and arsine ($AsH_3$) as products of the reductive HP, generated from either As(V) or As(III), are presented for the first time.

## EXPERIMENTAL SECTION

**Materials and Chemicals.** $TiO_2$ (AEROXIDE $TiO_2$ P25, Evonik) was used as received. Sodium meta-arsenite ($NaAsO_2$, Baker), sodium arsenate dibasic 7-hydrate ($Na_2HAsO_4{\cdot}7H_2O$, Baker), methanol (MeOH, 99.9%, for HPLC, Carlo Erba) and silver diethyldithiocarbamate ($(C_2H_5)_2NCSSAg$, Merck) were used. $HClO_4$ (70−72%, Merck) was employed for pH adjustments. All reagents were of the highest purity and used without further purification. Solutions and suspensions were prepared with deionized water (Apema Osmoion, resistivity = 18 MΩ cm).

**Photocatalytic Experiments.** Irradiations were performed in a quartz photoreactor well (Photochemical Reactors Ltd.) provided with a medium pressure mercury lamp (125 W, maximum emission at 366 nm, with minor emissions at 245, 254, 265, 280, 302, 313, 408, 436, and 546 nm), surrounded by a thermostatic jacket at 25 °C acting as IR filter. The lamp was previously switched on and stabilized for 30 min in another thermostatted jacket before insertion into the photoreactor well.

$TiO_2$ suspensions (180 mL) containing As(V) or As(III) at fixed concentrations without or with MeOH were ultrasonicated for 30 s, poured in the outer jacket of the well, and magnetically stirred and bubbled with $N_2$ (0.5 L $min^{-1}$) all throughout the reaction period. Strictly controlled anoxic conditions were used to avoid oxygen competition with As species. An initial stirring for 30 min in the dark was performed to reach the adsorption equilibrium of As species and donors onto $TiO_2$; the decrease of As concentration before switching on the lamp was discounted to establish the initial concentration in the HP experiments and take into account changes due only to light irradiation. As expected, no changes in As concentration were observed under irradiation in the absence of photocatalyst, since at 245 nm absorption of As species is very low and practically negligible at higher wavelengths.

Initial As(V) concentrations were 0.525, 0.065, and 0.013 mM, while those of As(III) were 0.525 and 0.013 mM; pH was initially adjusted to 3, unless indicated, and left to vary freely during the runs. $TiO_2$ concentration was always 1 g $L^{-1}$. 0.4 M MeOH was used; this concentration was chosen because it was the highest and optimal concentration used by Yang et al.,[7] and because our preliminary experiments showed no significant differences using MeOH in the 0.4−1.2 M range. Periodically, samples were taken from the suspensions and filtered through 0.2 μm Millipore membranes before analysis. UV spectra of filtered solutions did not present scattering, being good evidence that no $TiO_2$ particles came into solution. As it will be pointed out later, TEM images (Supporting Information (SI) Figure S2) indicated that particles aggregate in form of chains, not able to cross the filters.

All experiments were performed at least by duplicate and results averaged. The experimental error was never higher than 5%, as calculated by standard deviation among replicate experiments.

Actinometric measurements were made in the photoreactor well by the ferrioxalate method in the same conditions as the photocatalytic experiments. A photon flow per unit volume incident on the cell wall ($q^0_{n,p}/V$) of 127 μeinstein $s^{-1}$ $L^{-1}$ was calculated.

**Analytical Determinations in Filtered Samples.** Changes in As(V) concentration in solution were measured by spectrophotometry using the arsenomolybdate technique[35] (detection limit (DL): 0.01 mg $L^{-1}$). Total As in solution was determined by a modification of this method developed in our laboratory, as follows. To guarantee total As oxidation, excess potassium permanganate was added to the sample. After 75 min, reagents A and B of ref 35 were added, and spectrophotometric measurements were read only after 90 min contact time. In some few cases, total As was determined[36] by ICP-OES (DL: 0.005 mg $L^{-1}$, Perkin-Elmer Optima 5100 DV); a difference of only 3% was observed between both methods. Quantofix Arsen 10 strips (Macherey-Nagel) allowed detection and semiquantitative measurement of $AsH_3$ formed in the HP system. This test is a simplified Gutzeit method[37,38] that transform As species into $AsH_3$, which is then colorimetrically detected on the strip, and compared with a color scale. DL of this method is 0.01 mg $L^{-1}$. Quantitative $AsH_3$ determination was performed by the silver diethyldithiocarbamate spectrophotometric method (AgDDC, modified Gutzeit method),[39] adapting accordingly the photoreactor with a tight connection to the AgDDC setup. DL of this

method depends on the water composition and is between 0.0001 and 0.010 mg $L^{-1}$.[36] The reactor volume was decreased to 155 mL to avoid flooding into the tube containing the colorimetric reagent.

**Analysis of Solid Residues.** At the end of the HP runs, the solid residues were filtered and carefully dried under $N_2$. To test As(V) adsorbed onto the solids, powders were resuspended in deoxygenated 0.8% $NaHCO_3$, and As(V) was analyzed in the resulting solution.

For XRD analyses, a Philips PW-3710 diffractometer was used. For SEM-EDS analyses, a Fei Company Quanta 200 apparatus was employed. TEM images were obtained with a TEM-EM 301 Philips apparatus (60 kV). X-ray photoemission spectra (XPS) were taken with a hemispherical electrostatic energy analyzer ($r$ = 10 cm) using Al $K_\alpha$ radiation ($h\nu$ = 1486.6 eV). The binding-energy (BE) scale was calibrated with the $TiO_2$ $Ti2p_{3/2}$ peak position, placed at 458.5 eV.[40] X-ray absorption near edge spectroscopy (XANES) analyses were performed using the in-house X-ray absorption spectrometer, Rigaku R-XAS Looper. As K-edge and Au L3-edge X-ray XANES spectra were measured at room temperature in the transmission mode. For experiments starting from As(V), a fluorescence detector was employed. A Si(620) single crystal was used to obtain a monochromatic incident beam from a Mo anode target, using a current of 50 mA in the filament and a high voltage of 50 kV in the tube. Intensities of incident and transmitted X-rays were measured using an argon-filled proportional counter and a scintillation counter, respectively. XAS spectra were collected from 11800 to 11950 eV in steps of 1 eV, reduced to 0.2 eV in the XANES region (11840−11920 eV). The incident photon energy was calibrated using the first inflection point of the Au L3-edge (11919.7 eV) for measurements at the As K-edge (11867 eV). Ten spectra were taken with exposure times of 4 h each one. The data treatment was performed by subtracting the pre-edge background followed by normalization by extrapolation of a quadratic polynomial fitted at the post-edge region of the spectrum.

## RESULTS

**As(V) Photocatalytic Experiments.** In Figure 1, results of experiments with As(V) (0.525 mM, pH 3) over $TiO_2$ are shown. At pH 3, forms for As(V) and As(III) are predominantly $H_2AsO_4^-$ and $As(OH)_3$. A decay of only 3−7% of the As(V) initial concentration was measured after 30 min stirring in the dark. In the absence of MeOH, As(V) concentration did not change during the run (not shown), but the decay was evident when 0.4 M MeOH was added, reaching an almost total As(V) removal at ca. 150 min. A slight increase (<0.5 units) in pH was observed during the experiments. At the end of the run, a grayish solid layer was found onto the $TiO_2$ surface, suggesting the formation of As(0) in its most stable allotropic form ($\alpha$) at room temperature.[41] Similar findings were reported by Yang et al. but not many details were given by the authors.[7] In same Figure 1, evolution of total As in solution is plotted, from which As(III) was calculated. As(III) increased steadily, but around 90 min, when As(V) was almost totally depleted, As(III) began to decay, indicating that this species is also photocatalytically transformed, in accordance with results obtained in the As(III) HP system (see next section). Assuming that As(0) was the only other species formed in high amount (see below for $AsH_3$ production), its evolution was calculated by mass balance, showing a clear increase

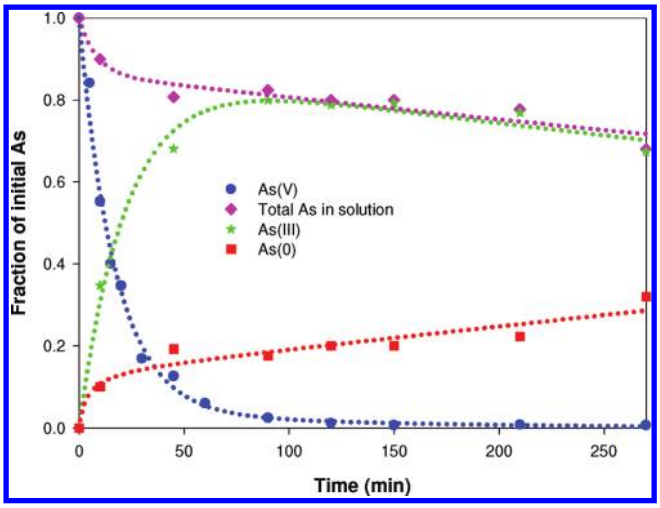


**Figure 1.** Temporal evolution of As species under light irradiation over $TiO_2$ in the presence of MeOH starting from As(V). Conditions: $[As(V)]_0$ = 0.525 mM, [MeOH] = 0.4 M, $[TiO_2]$ = 1 g $L^{-1}$, pH 3, experiments under $N_2$ (0.5 L $min^{-1}$), $\lambda_{max}$ = 366 nm, $q^0_{n,p}/V$ = 127 $\mu$einstein $s^{-1}$ $L^{-1}$, $T$ = 25 °C. Dotted lines are only for better visualization of the experimental points.

with time. Interestingly, data at 270 min indicate still the presence of 68% of As in solution, in the form of As(III).

Analysis with the Quantofix strips allowed $AsH_3$ detection in the headspace of the photoreactor. At 270 min, $AsH_3$ amounted to roughly 0.025 mg $L^{-1}$ (ca. 0.06% of the initial As). A separate experiment was performed up to 160 min for a more strict $AsH_3$ quantification with AgDDC; $AsH_3$ began to be detected at 135 min, and 3.9 × $10^{-4}$ mM were measured at 160 min, indicating that only ca. 0.07% of the initial As was transformed into $AsH_3$.

Similar HP experiments starting from lower As(V) concentrations revealed interesting findings. With 0.065 mM, removal was 82% after 30 min in the dark (much higher than that obtained with 0.525 mM, in accordance with Pena et al.);[13] as no darkening of the photocatalyst was observed, this indicates clearly that the decrease was due only to an adsorption process. However, after 30 min more under irradiation, 90% As(V) removal was achieved, and the gray deposit attributed to As(0) was observed over the photocatalyst, together with $AsH_3$ evolution. When starting from 0.013 mM As(V), 82% removal was observed after 30 min in the dark. After 30 min more under irradiation, As(0) appearance and $AsH_3$ evolution also took place, while As remaining in solution was below 10 $\mu$g $L^{-1}$. These results are clearly indicative that reductive pathways took place under irradiation.

**As(III) Photocatalytic Experiments.** Experiments starting from As(III) (0.525 mM, 0.4 M MeOH, pH 3) are shown in Figure 2(a). No adsorption was observed after 30 min in the dark, consistent with the neutral form of As(III) at the working pH and concentration. After 195 min of irradiation, 38% As(III) was removed, with an increase of pH not higher than 0.5 units. Similar results were obtained with 0.2 and 0.8 M MeOH (not shown). As(V) was not found in solution. Although As(V) was detected in traces in the solid residue after desorption with $NaHCO_3$, its quantification in solution was erratic due to the low concentration. Figure 2(a) also shows that As(III) decays at a lower rate than As(V) in Figure 1, with a totally different kinetic profile. As(0) was deposited on the catalyst; a mass balance (neglecting adsorbed As(V) and $AsH_3$)


dx.doi.org/10.1021/es202638c | Environ. Sci. Technol. 2012, 46, 2299−2308

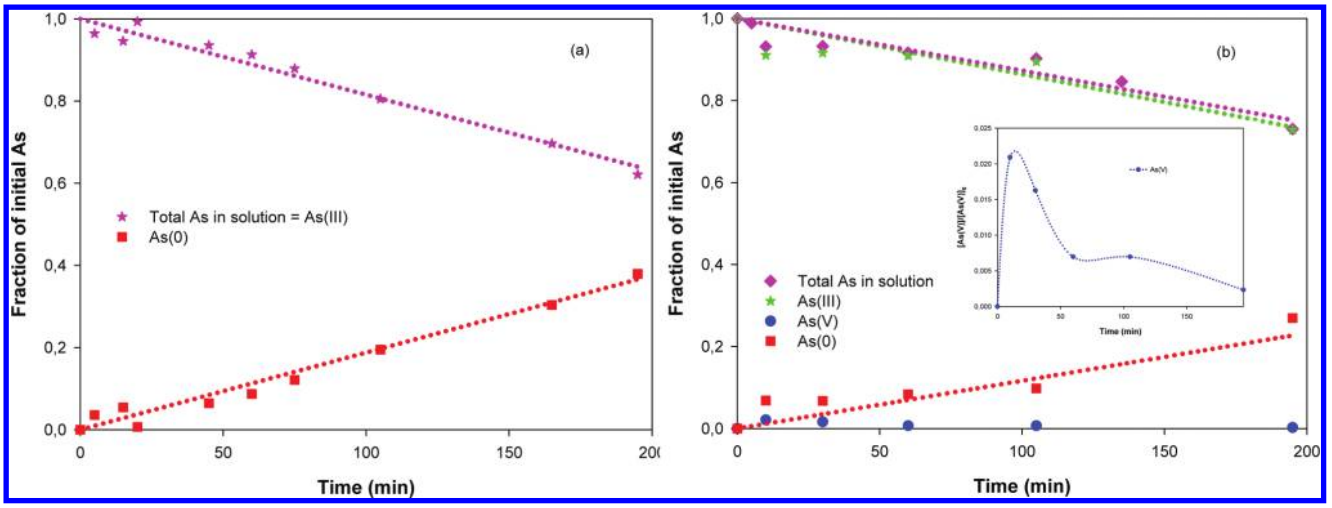


**Figure 2.** Temporal evolution of As species under light irradiation over $TiO_2$ starting from As(III), (a) in the presence of 0.4 M MeOH, (b) in the absence of MeOH. Same conditions of Figure 1, except $[As(III)]_0$ = 0.525 mM. Dotted lines are only for better visualization of the experimental points.

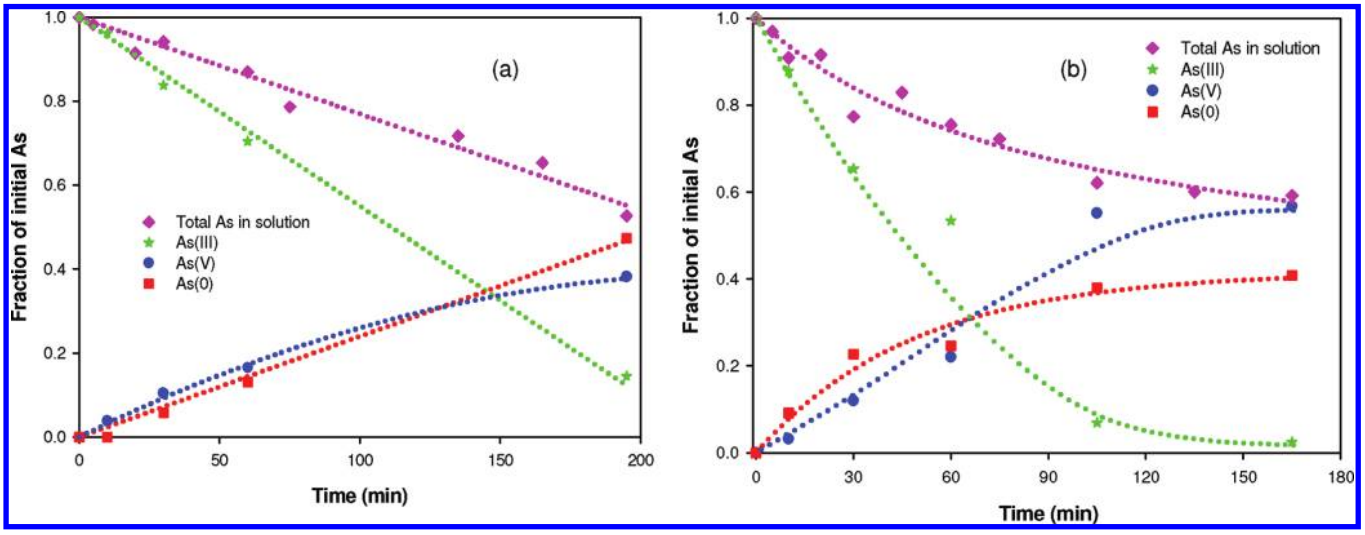


**Figure 3.** Temporal evolution of As species under light irradiation over $TiO_2$ starting from As(III), (a) in the presence of 0.4 M MeOH, (b) in the absence of MeOH. Similar conditions of Figure 1, except $[As(III)]_0$ = 0.525 mM, pH 10. Dotted lines are only for better visualization of the experimental points.

indicates an increase up to ca. 38% at 195 min. $AsH_3$ evolved initially at 30 min; at 135 min, Quantofix strips indicated the maximum $AsH_3$ concentration possible to be measured by this method (0.5 mg $L^{-1}$, 1.2% of the initial As), that is, a rather higher production than in the As(V) system.

A similar experiment starting from 0.013 mM As(III) yielded more than 90% As removal in the dark after initial contact with the photocatalyst, without evidence of gray deposits onto $TiO_2$. After 30 min more under irradiation, As(0) formation was observed, together with $AsH_3$ evolution, leaving less than 10 $\mu$g As $L^{-1}$ in solution.

Figure 2(b) shows similar experiments but in the absence of MeOH. Interestingly, in contrast with the total lack of reaction of As(V) in the absence of donor, a rather important decay of As(III) (similar to that of total As) was observed in these conditions, although somewhat lower than in the presence of MeOH (27% vs 38% in 195 min, respectively). In this case, As(V) was actually detected in solution: the maximum quantity, ca. 2%, was found at 10 min, followed by a decrease (Figure 2(b), inset), which could be attributed to adsorption onto $TiO_2$. In agreement, As(V) desorbed from the photocatalyst was detected in traces. Figure 2(b) shows also As(0) formation. $AsH_3$ was detected at 45 min; ca. 0.01 mg $L^{-1}$ (0.02% of the initial As) were found at 135 min, that is, a much lower concentration than in the presence of MeOH, reaching 0.1 mg $L^{-1}$ only at 195 min. A separate experiment for AgDDC measurement indicated that at 60 min 0.06% of As had been transformed into $AsH_3$.

Other experiments were performed with 0.525 mM As(III) but without $HClO_4$ addition (pH 10) to verify that for As(III) transformation into As(0) and $AsH_3$ only $TiO_2$ and light are needed, and to discard any possible effect of $HClO_4$. At pH 10, As(III) (mainly as $H_2AsO_3^-$) and $TiO_2$ are negatively charged, and hence no As(III) adsorption was observed in the dark. In the presence of MeOH, As(III) decay was high (86%). Total As decayed faster than at pH 3 (47 vs 38%, respectively, cf. Figures 2(a) and 3(a)). As(V) and As(0) were produced here appreciably, both species being formed at similar rates in the first stages; an arrest on the rate of As(V) evolution took place around 100 min. $AsH_3$ appeared at 35 min and reached 0.5 mg $L^{-1}$


dx.doi.org/10.1021/es202638c | Environ. Sci. Technol. 2012, 46, 2299–2308

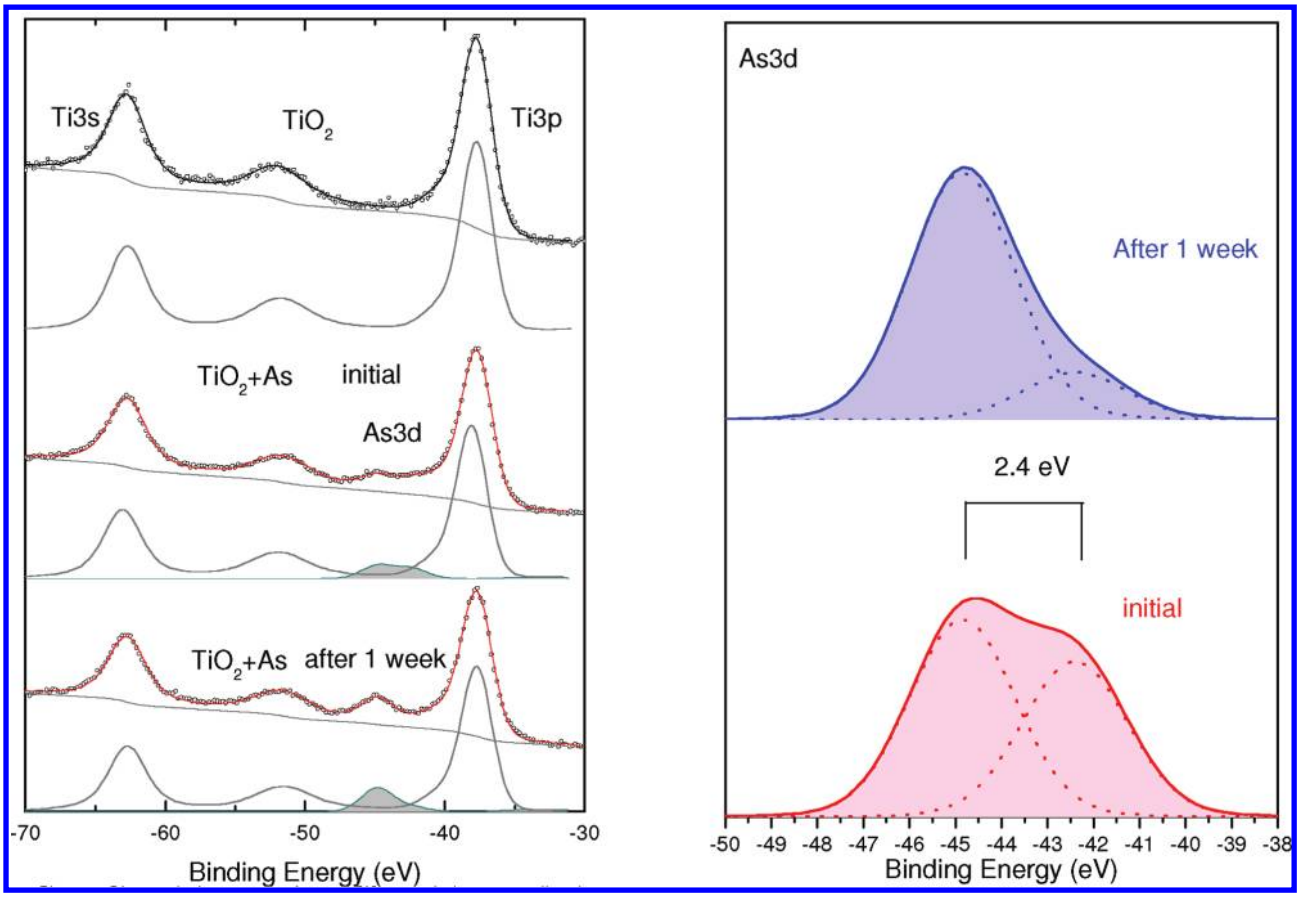


**Figure 4.** Left: photoemission spectra of pure P25 (upper panel) and samples after a HP experiment (0.525 mM As(V), 0.4 M MeOH, pH 3). Middle panel: sample taken approximately 48 h after the end of the run; lower panel: sample taken after 1 week in air. Black lines: best fittings of the spectra; gray lines: components used for the fits. Right: As3d components corresponding to the fittings of the spectra acquired 48 h after insertion of HP samples in the analysis chamber (red) and after 1 week (blue). Dotted lines: subcomponents assigned to As(0) and As(III), at low and high BE, respectively.

(1.3% of the initial As) at 105 min, being the highest amount produced in all HP systems. Note that the calculation of As(0) by mass balance is not totally correct in this case because of the rather considerable $AsH_3$ production in the last stages. In contrast with experiments at pH 3, pH decreased from 10 to 8.

Figure 3(b) shows the results in the absence of MeOH. Total As decayed to ca. 40%, somewhat less than in the presence of MeOH (cf. Figure 3(a) and (b)). As(V) in solution and As(0) were appreciably produced with similar formation rates in the first stages. However, after 60 min, As(V) increased very rapidly and was the only species in solution at the end of the experiment, implying a total As(III) oxidation. $AsH_3$ appeared at 20 min and the maximum concentration reached was around 0.4 mg $L^{-1}$ (1.0% of the initial As) at 195 min; note that a similar concentration was found sooner (at 105 min) in the presence of MeOH. 41% of As(0) was formed, although this value is also affected by error because of the high $AsH_3$ production in the last stages. pH decrease was higher than in the presence of MeOH (from 10 to 7).

**Analysis of Solid Residues.** Dark residues, attributed to As(0), were deposited on $TiO_2$ after the HP reactions, and whitened gradually with time, indicating oxidation to arsenic oxides in air. XRD patterns (not shown) corresponded always to P25, without As signals, due probably to the low amount or to the lack of crystallinity of the deposits. SEM images (SI Figure S1) showed that the deposit was composed of nanoparticles, while the EDS analysis revealed that it contained As in a $TiO_2$ matrix. TEM images (SI Figure S2) indicate a particle size between 10 and 15 nm, disposed in chain form. A comparison with pure P25 (not shown) demonstrated no appreciable differences, indicating that the reaction took place without morphology changes.

The oxidation state of As in the deposits was determined by XPS. Figure 4 (left) presents three spectra in the region of the As 3d peak. The upper spectrum corresponds to pure P25, whereas the other two spectra correspond to the deposit at the end of a HP experiment (0.525 mM As(V), 0.4 M MeOH, pH 3). The spectrum in the middle panel was taken approximately 48 h after the end of the experiment, while that in the lower panel was taken after around 1 week in air. The spectra are dominated by the Ti 3p and 3s peaks at 37.7 and 62.9 eV, respectively; a satellite of the Ti3p peak is also clearly visible at 14 eV larger BE. The spectrum in the middle panel shows a weak but clear increase of intensity in the region between 42 and 44 eV, where the As3d contribution is expected. In the spectrum after one week, this contribution is more apparent and more concentrated in the region around 44 eV. Isolation and comparison of As contributions can be viewed in Figure 4 (left), where the resulting fits are shown, together with the components used in each case (See SI). The fits of the last two spectra yield different As3d components, compared in more detail in Figure 4 (right). It is concluded that initially there are similar amounts of As(0) and As(III); after 1 week in air, the

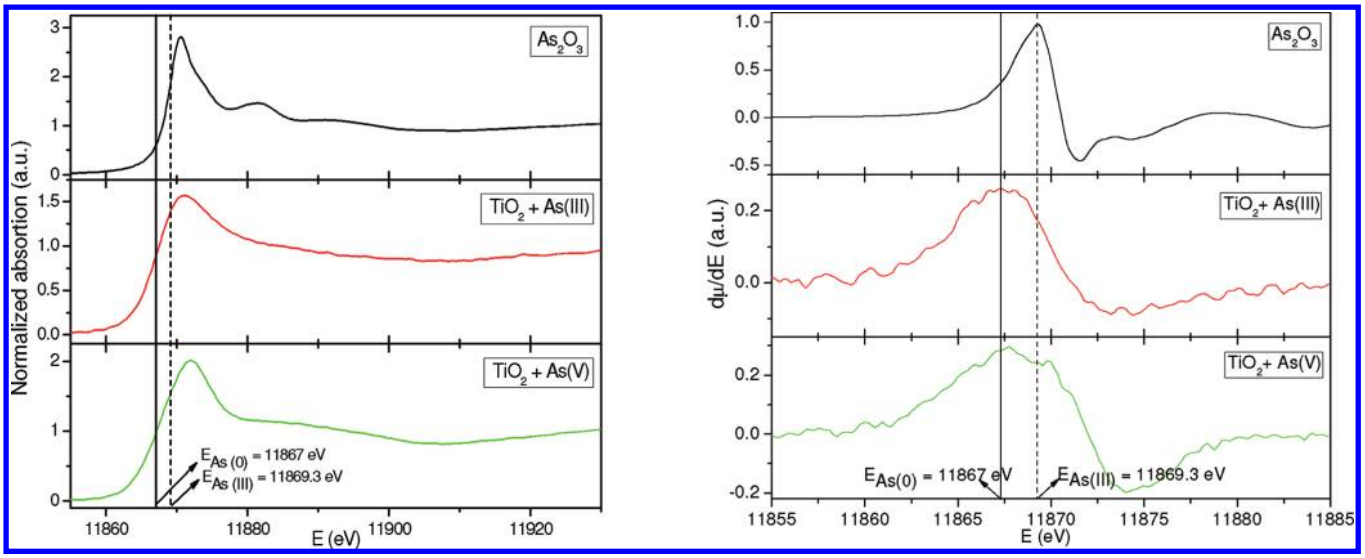


**Figure 5.** Normalized As−K XANES spectra of solids obtained from HP experiments in the presence of 0.4 M MeOH (0.525 mM As(III), pH 10 (middle) and 0.525 mM As(V), pH 3 (down)). Left: row data; right: first derivatives of the spectra to clearly show the absorption edge position for the HP samples. Full vertical line: position for the reported energy edge (maximum at the first derivative spectrum) for As(0) species; dotted vertical line: As(III) species.

amount of As(0) was strongly reduced in favor of the As oxidized species.

XAS studies performed at the As K-edge[42,43] gave more information on the average As oxidation states. Figure 5 (left) shows the XANES spectra of the solids obtained after HP experiments in the presence of MeOH. The spectrum in the middle panel corresponds to a run with 0.525 mM As(III) at pH 10, and that in the lower panel corresponds to a run with 0.525 mM As(V) at pH 3; the spectrum of $As_2O_3$ as reference appears in the upper panel. The values of the edge absorption energies were obtained from the maximum in the first derivative of each spectrum (Figure 5 (right)). For the sample coming from As(III), the absorption edge was at 11867.4 eV, close to the As(0) reported value.[44−46] The obtained weak white line (first maximum of the absorption spectrum), compared with the intense one expected for $As_2O_3$, confirms reduction of As(III) to As(0). On the other hand, the spectrum of the sample coming from As(V) presents an absorption edge energy of 11868.7 eV, corresponding to an intermediate value between those reported for As(0) and As(III);[47] the final product can be assigned to a mixture of these species, and the existence of some As(V) cannot be ruled out. The presence of more than one As species in that sample is consistent with the increment on the white line of the spectrum, traduced by a broader maximum in its derivative spectrum. Radiation damage (i.e., oxidation of As(III)) could be discarded since the experiments were performed in an "in-house" spectrometer with a lower photon flux than that used in a synchrotron laboratory. Additionally, successive XANES spectra were recorded to verify the stability of the As state.[44]

## DISCUSSION

**Mechanisms at Acid pH.** As said before, direct As(V) reduction by P25 $e_{CB}^-$ is not possible but an indirect reductive mechanism would be possible in the presence of electron donors. Generation of strong reducing hydroxymethyl radicals ($^\bullet CH_2OH$) from MeOH by $h_{VB}^+/HO^\bullet$ attack (eqs 5 and 5′), is thermodynamically possible ($E^0$ ($^\bullet CH_2OH/CH_3OH$) = 1.45 V).[48] In the absence of $O_2$, $^\bullet CH_2OH$ can donate electrons to the CB (current doubling effect, eq 6) or be the effective As(V) reductant, with formaldehyde generation (eq 7). The reduction potential of $^\bullet CH_2OH$ to $CH_2O$ ($E^0 \approx -0.90$ to $-1.18$ V)[33] is in the limit for As(V) reduction to As(IV), but the value may be somewhat more negative on the $TiO_2$ surface at pH 3.

$$CH_3OH + h_{VB}^+\{HO^\bullet\} \rightarrow {}^\bullet CH_2OH + H^+\{H_2O\} \quad (5, 5')$$

$$^\bullet CH_2OH \rightarrow CH_2O + H^+ + e_{CB}^- \quad (6)$$

$$^\bullet CH_2OH + As(V) \rightarrow CH_2O + As(IV) + H^+ \quad (7)$$

In the HP system, formaldehyde can be transformed to formic acid (FA) and finally mineralized to $CO_2$. FA generates a much stronger reducing agent, $CO_2^{\bullet-}$ ($E^0$ ($CO_2/CO_2^{\bullet-}$) $\approx -2.0$ V),[33] which is a better current doubling agent and can contribute to the reducing process of As(V).

$$CH_2O \rightarrow HCOOH \rightarrow CO_2 \quad (8)$$

$$HCOOH + h_{vb}^+\{HO^\bullet\} \rightarrow CO_2^{\bullet-} + 2H^+\{H_3O^+\} \quad (9)$$

$$CO_2^{\bullet-} + As(V) \rightarrow CO_2 + As(IV) \quad (10)$$

Experiments in solution of our laboratory not reported yet, irradiating ($\lambda$ > 300 nm) a mixture of $KNO_3$ (used as $HO^\bullet$ producer)[49] and MeOH under $N_2$, produced an immediate As(V) depletion, confirming that reducing radicals in solution are the species responsible for As(V) reduction and that $TiO_2$ is not necessary; a more profound analysis of this system is underway.

As(IV) is easily reduced to As(III)[19,34] by CB or trapped[50] electrons (reaction 11), by $^\bullet CH_2OH$ (reaction 11′) or by the equivalent reaction with $CO_2^{\bullet-}$ (not shown):

$$As(IV) + e_{CB}^-/e_{trapp}^-\{^\bullet CH_2OH\} \rightarrow As(III)\{CH_2O + H^+\} \quad (11, 11')$$


dx.doi.org/10.1021/es202638c | Environ. Sci. Technol. 2012, 46, 2299−2308

**Scheme 1. Energy Diagram of the As(V)/As(III) Reductive HP System at Acid pH Showing the Standard Reduction Potentials of the Involved Couples[a]**

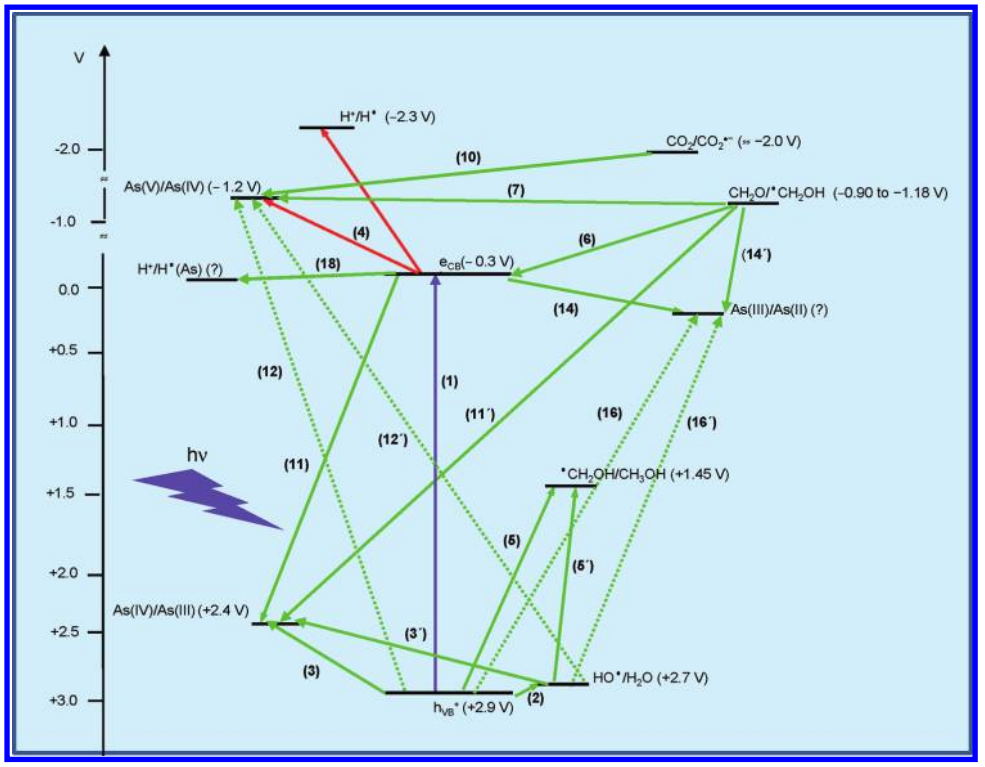


[a]The numbers in bold correspond to some of the equations. Red lines: forbidden processes. Dotted lines: less possible processes in the presence of MeOH.

At the high MeOH concentrations used (0.4 M), reactions 5, 5′, would be preferred over competing As(IV) reoxidation:

$$\mathrm{As(IV)} + \mathrm{h_{VB}}^{+}\{\mathrm{HO}^{\bullet} + \mathrm{H}^{+}\} \rightarrow \mathrm{As(V)}\{\mathrm{H_2O}\} \qquad (12,\ 12')$$

As(IV) can also rapidly disproportionate,[11,34] process enhanced over $TiO_2$:[16]

$$2\mathrm{As(IV)} \rightarrow \mathrm{As(III)} + \mathrm{As(V)} \qquad (13)$$

Once formed, As(III) can be also photocatalytically reduced (Figures 1 and 2(a)). However, As(III) reduction can actually take place in the absence of MeOH (Figure 2(b)), oppositely to As(V). Assuming one-electron consecutive steps, As(III) reduction with would lead first to As(II), an unstable oxidation state, whose $E^0$ is unknown, but already postulated in the radiolysis of oxygen-free arsenite:[51,52]

$$\mathrm{As(III)} + \mathrm{e_{CB}}^{-}/\mathrm{e_{trapp}}^{-}\{^{\bullet}\mathrm{CH_2OH}\} \rightarrow \mathrm{As(II)}\{\mathrm{CH_2O} + \mathrm{H}^{+}\} \qquad (14,\ 14')$$

(or equivalent reaction with $CO_2^{\bullet-}$)

Successive one-electron transfer and/or disproportionation reactions would lead to the formation of stable products such as As(0) and $AsH_3$. As(0) formation has been reported in radiolytic deoxygenated arsenite experiments.[52]

In the absence of MeOH, As(III) HP reduction is somewhat less efficient (cf. Figures 2(a) and (b)) because the anodic reaction is the sluggish oxidation of water by $h_{VB}^{+}$:[5,6]

$$2\mathrm{H_2O} + 4\mathrm{h_{VB}}^{+} \rightarrow \mathrm{O_2} + 4\mathrm{H}^{+} \qquad (15)$$

Competition of As(II) for the charge carriers would lead to unproductive short-circuiting and reoxidation to As(III):

$$\mathrm{As(II)} + \mathrm{h_{VB}}^{+}\{\mathrm{HO}^{\bullet} + \mathrm{H}^{+}\} \rightarrow \mathrm{As(III)}\{\mathrm{H_2O}\} \qquad (16,\ 16')$$

In the absence of MeOH, and in contrast with the same reaction in the presence of the donor, As(III) can be not only reduced through reaction 14, but also easily oxidized to As(IV) through reactions 3, 3′, because it is an effective $HO^{\bullet}$ ($k = 9 \times 10^9\ M^{-1}\ s^{-1}$) and hole scavenger;[19] traces of $O_2$ produced through reaction 15 would enhance oxidation. This leads ultimately to As(V) formation through reactions 12, 12′, and 13 or by injection of electrons to the CB (eq 17), explaining the formation of low amounts of As(V) in the system (Figure 2(b)), a process not taking place appreciably when MeOH is present (Figure 2(a)).

$$\mathrm{As(IV)} \rightarrow \mathrm{As(V)} + \mathrm{e_{CB}}^{-} \qquad (17)$$

In other studies,[9−11,13,15,16,19,22] the low but observable As(V) formation in HP-As(III) deoxygenated systems was not carefully examined and only associated to the action of residual $O_2$, adsorbed or present in the crystalline lattice of the photocatalyst.

In all cases, the system conditions will become rather reducing, for example, by the formation of $AsH_3$ and As(IV), both rather good reducing species.[34,41]

$H^+$ reduction to $H^{\bullet}$, ending in $H_2$, can be another reducing source. Though $H_2$ was not detected in the present case, a low concentration is expected because $H^{\bullet}$ and $H_2$ would be rapidly consumed, forming, for example, $AsH_3$,[53] or reducing As(V) and As(III) to As(0).[41] $H^+$ reduction is thermodynamically and kinetically restricted on bare P25 ($E^0(H^+/H^{\bullet}) = -2.3$ V,[54] a value probably lower on the $TiO_2$ surface). However, the


dx.doi.org/10.1021/es202638c | Environ. Sci. Technol. 2012, 46, 2299−2308

reaction can be assisted by small spots of nanosized As(0), with formation of a Schottky barrier of ca. 0.9 eV at the As/$TiO_2$ interface (work functions for As(0) and P25 are 5.1 eV[55] and 4.2 eV,[56,57] respectively), enabling electrons to flow from $TiO_2$ to As(0):[58]

$$H^+(As(0)) + e_{CB}^- \rightarrow H^\bullet(As(0)) \quad (18)$$

$$2H^\bullet(As(0)) \rightarrow H_2 \quad (19)$$

$$H^\bullet(As(0)) + CH_3OH \rightarrow As(0) + H_2 + {}^\bullet CH_2OH \quad (20)$$

In Scheme 1, an energy diagram of the HP system is shown, indicating all possible processes.

At a certain extent, deposited As(0) (which amounts more than 1% on the $TiO_2$ surface at the end of the experiments) and $AsH_3$, known to be poisoning agents in catalytic reactions,[46,59] may deactivate the surface by blocking active sites.

**Effect of pH.** The global reactions from As(V) to As(III), As(0) and $AsH_3$ in the presence of MeOH at acid pH proceed with increase of pH (SI eqs S1−S3), whereas those from As(III) (SI eqs S4−S7) proceed without pH changes. In the experiments of this work, pH changes were almost negligible, indicating the complexity of the systems.

The enhancement of As(III) decay at pH 10 (Figure 3(a) and (b)) can be explained by three reasons: (1) the level of the CB is negatively shifted, making more favorable the direct As(III) reduction (provided the As(III)/As(II) couple does not depend on pH); (2) the reducing radical of MeOH is mostly in the anionic form ($^\bullet CH_2O^-$, $pK_a$ = 10.7),[60] a more powerful reductant ($E^0 \approx -1.60-1.81$ V)[33] than its precursor; (3) an enhancement of oxidative pathways occurs, with formation of As(IV) and As(V) through reactions 3, 3′, 12, 12′, 13, and 17. Reasons (1) and (2) would explain the higher As(0) and $AsH_3$ yields compared with those at pH 3, and (3) is particularly important in the absence of MeOH, because As(V) will be produced by immediate capture of $h_{VB}^+$ or $HO^\bullet$ (in part as $O^{\bullet-}$, $pK_a$ = 11.9),[61] by As(IV) through reactions 12 and 12′, favored by the alkaline medium and a higher $O_2$ production due to reaction 21, or through reactions 13 or 17.

$$4HO^- + 4h_{VB}^+ \rightarrow O_2 + 2H_2O \quad (21)$$

Furthermore, a higher release of As(V) in solution is expected at pH 10 due to negligible As(V) adsorption and/or a more favorable desorption, as both As(V) (mainly as $HAsO_4^{2-}$) and $TiO_2$ are negatively charged.

The decrease of pH observed in both alkaline systems, especially in the absence of MeOH, is explained because As(V) formation by As(III) oxidation consumes hydroxyls (SI eqs S12 and S13).

The deceleration of As(V) production in solution at ca. 150 min in the presence of MeOH (Figure 3(a)) can be ascribed to As(III) reduction by $^\bullet CH_2O^-$, or to As(V) reduction by the effect of the electron donor. However, this decay is also visible in the absence of the alcohol (Figure 3(b)), but here it should be ascribed to depletion of As(III) from which As(V) is rapidly formed through reactions 3, 3′ and 12, 12′, As(V) being the only final species in solution.

**Environmental Implications.** As observed, As(III) HP reduction is possible in deoxygenated suspensions. As(V) can be also reduced, but only in the presence of an electron donor such as MeOH. In all cases, As(0) and $AsH_3$ are formed. The reductive HP process is very efficient at the lowest As (III or V) concentrations (e.g., 0.013 mM ≡ 1 mg $L^{-1}$, a common value found in natural polluted groundwaters) because As levels in agreement with drinking water regulations (<10 $\mu$g $L^{-1}$)[3] were attained.

As(0) formation results a definite way to make less mobile As(V) and As(III) species present in aqueous media. However, it is important to remark that $AsH_3$, a very toxic compound, is formed in these HP systems, and use of a fume hood is mandatory. Some strategies to remove or contain $AsH_3$ are envisaged: (1) adsorption on suitable catalysts,[62,63] or (2) treatment by a second $TiO_2$ photocatalytic oxidative step in the gas phase using supported $TiO_2$. This will be the subject of future research.

## ■ ASSOCIATED CONTENT

### Ⓢ Supporting Information

SEM and TEM images, additional XPS information, and global reaction equations. This material is available free of charge via the Internet at http://pubs.acs.org.

## ■ AUTHOR INFORMATION

### Corresponding Author

*E-mail: litter@cnea.gov.ar.

## ■ ACKNOWLEDGMENTS

This work was performed as part of Agencia Nacional de Promoción Científica y Tecnológica PICT-512, PICT-2008-00038, PAE-PME-2007-00039, PICT 33432 and CYTED 406RT0282 Thematic Network. To Dr. Alejandro Senn and Dr. Martín Meichtry for helpful discussions.

## ■ REFERENCES

(1) Litter, M. I.; Morgada, M. E.; Bundschuh, J. Possible treatments for arsenic removal in Latin American waters for human consumption. *Environ. Pollut.* **2010**, *158*, 1105−1118.

(2) Bundschuh, J.; Litter, M.; Ciminelli, V.; Morgada, M. E.; Cornejo, L.; Garrido Hoyos, S.; Hoinkis, J.; Alarcón-Herrera, M. T.; Armienta, M. A.; Bhattacharya, P. Emerging mitigation needs and sustainable options for solving the arsenic problems of rural and isolated urban areas in Iberoamerica—A critical analysis. *Water Res.* **2010**, *44*, 5828−5845.

(3) *Guidelines for Drinking Water Quality. Recommendations*, 3rd ed.; World Health Organization: Geneva, 2004; Vol. *1*.

(4) Hoffmann, M. R.; Martin, S. T.; Choi, W.; Bahnemann, D. W. Environmental applications of semiconductor photocatalysis. *Chem. Rev.* **1995**, *95*, 69−96.

(5) Litter, M. I. Heterogeneous Photocatalysis. Transition metal ions in photocatalytic systems. *Appl. Catal. B* **1999**, *23*, 89−114.

(6) Litter, M. I. Treatment of chromium, mercury, lead, uranium and arsenic in water by heterogeneous photocatalysis. *Adv. Chem. Eng.* **2009**, *36*, 37−67.

(7) Yang, H.; Lin, W. -Y.; Rajeshwar, K. Homogeneous and heterogeneous photocatalytic reactions involving As(III) and As(V) species in aqueous media. *J. Photochem. Photobiol., A* **1999**, *123*, 137−143.

(8) Bissen, M.; Vieillard-Baron, M. M.; Schindelin, A. J.; Frimmel, F. H. $TiO_2$-catalyzed photooxidation of arsenite to arsenate in aqueous samples. *Chemosphere* **2001**, *44*, 751−757.

(9) Lee, H.; Choi, W. Photocatalytic oxidation of arsenite in $TiO_2$ suspension: Kinetics and mechanisms. *Environ. Sci. Technol.* **2002**, *36*, 3872−3878.

(10) Jayaweera, P. M.; Godakumbra, P. I.; Pathiartne, K. A. S. Photocatalytic oxidation of As(III) to As(V) in aqueous solutions: A low cost pre-oxidative treatment for total removal of arsenic from water. *Curr. Sci. India* **2003**, *84*, 541−543.

(11) Ryu, J.; Choi, W. Effects of $TiO_2$ surface modifications on photocatalytic oxidation of arsenite: The role of superoxides. *Environ. Sci. Technol.* **2004**, *38*, 2928−2933.
(12) Dutta, P. K.; Pehkonen, S. O.; Sharma, V. K.; Ray, A. K. Photocatalytic oxidation of arsenic(III): Evidence of hydroxyl radicals. *Environ. Sci. Technol.* **2005**, *39*, 1827−1834.
(13) Pena, M. E.; Korfiatis, G. P.; Patel, M.; Lippincott, L.; Meng, X. Adsorption of As(V) and As(III) by nanocrystalline titanium dioxide. *Water Res.* **2005**, *39*, 2327−2337.
(14) Ferguson, M. A.; Hoffmann, M. R.; Hering, J. G. $TiO_2$-photocatalyzed As(III) oxidation in aqueous suspensions: Reaction kinetics and effects of adsorption. *Environ. Sci. Technol.* **2005**, *39*, 1880−1886.
(15) Yoon, S.; Lee, J. H. Oxidation mechanism of As(III) in the UV/$TiO_2$ system: Evidence for a direct hole oxidation mechanism. *Environ. Sci. Technol.* **2005**, *39*, 9695−9701.
(16) Xu, T.; Kamat, P. V.; O'Shea, K. E. Mechanistic evaluation of arsenite oxidation in $TiO_2$ assisted photocatalysis. *J. Phys. Chem. A* **2005**, *109*, 9070−9075.
(17) Zhang, F. -S.; Itoh, I. Photocatalytic oxidation and removal of arsenite from water using slag-iron oxide-$TiO_2$ adsorbent. *Chemosphere* **2006**, *65*, 125−131.
(18) Ferguson, M. A.; Hering, J. G. $TiO_2$-photocatalyzed As(III) oxidation in a fixed-bed, flow-through reactor. *Environ. Sci. Technol.* **2006**, *40*, 4261−4267.
(19) Ryu, J.; Choi, W. Photocatalytic oxidation of arsenite on $TiO_2$: Understanding the controversial oxidation mechanism involving superoxides and the effect of alternative electron acceptors. *Environ. Sci. Technol.* **2006**, *40*, 7034−7039.
(20) Leng, W. H.; Cheng, X. F.; Zhang, J. Q.; Cao, C. N. Comment on "Photocatalytic oxidation of arsenite on $TiO_2$: Understanding the controversial oxidation mechanism involving superoxides and the effect of alternative electron acceptors. *Environ. Sci. Technol.* **2007**, *41*, 6311−6312.
(21) Fostier, A. H.; Silva Pereira, M. S.; Rath, S.; Guimaraẽs, J. R. Arsenic removal from water employing heterogeneous photocatalysis with $TiO_2$ immobilized in PET bottles. *Chemosphere* **2008**, *72*, 319−324.
(22) Yoon, S.; Oh, S.-E.; Yang, J. E.; Yu, S.; Pak, D. $TiO_2$ photocatalytic oxidation mechanism of As(III). *Environ. Sci. Technol.* **2009**, *43*, 864−869.
(23) Li, Q.; Easter, N. J.; Shang, J. K. As(III) removal by palladium-modified nitrogen-doped titanium oxide nanoparticle photocatalyst. *Environ. Sci. Technol.* **2009**, *43*, 1534−1539.
(24) Tsimas, E. S.; Tyrovola, K.; Nikolaos P. Xekoukoulotakis, N. P.; Nikolaidis, N. P.; Diamadopoulos, E.; Mantzavinos, D. Simultaneous photocatalytic oxidation of As(III) and humic acid in aqueous $TiO_2$ suspensions. *J. Hazard. Mater.* **2009**, *169*, 376−385.
(25) Nguyen, T. V.; Vigneswaran, S.; Ngo, H. H.; Kandasamy, J.; Choi, H. C. Arsenic removal by photo-catalysis hybrid system. *Sep. Purif. Technol.* **2008**, *61*, 44−50.
(26) Sharma, V. K.; Sohn, M. Aquatic arsenic: Toxicity, speciation, transformations, and remediation. *Environ. Int.* **2009**, *35*, 743−759.
(27) Xu, Z.; Meng, X. Size effects of nanocrystalline $TiO_2$ on As(V) and As(III) adsorption and As(III) photooxidation. *J. Hazard. Mater.* **2009**, *168*, 747−752.
(28) Morgada de Boggio, M. E.; Levy, I. K.; Mateu, M.; Bhattacharya, P.; Bundschuh, J.; Litter, M. I. Low-cost technologies based on heterogeneous photocatalysis and zerovalent iron for arsenic removal in the Chacopampean plain, Argentina. In *Natural Arsenic in Groundwater of Latin America—Occurrence, health impact and remediation*; Bundschuh, J., Armienta, M. A., Bhattacharya, P., Matschullat, J., Birkle, P., Mukherjee, A. B., Eds.; Balkema Publisher: Lisse, 2010; pp 677−686.
(29) Choi, W.; Yeo, J.; Ryu, J.; Tachikawa, T.; Majima, T. Photocatalytic oxidation mechanism of As(III) on $TiO_2$: Unique role of As(III) as a charge recombinant species. *Environ. Sci. Technol.* **2010**, *44*, 9099−9104.
(30) Litter, M. I.; Alarcón-Herrera, M. T.; Arenas, M. J.; Armienta, M. A.; Avilés, M.; Cáceres, R. E.; Cipriani, H. N.; Cornejo, L.; Dias, L. E.; Fernández Cirelli, A.; Farfán, E. M.; Garrido, S.; Lorenzo, L.; Morgada, M. E.; Olmos-Márquez, M. A.; Pérez-Carrera, A. Small-scale and household methods to remove arsenic from water for drinking purposes in Latin America. *Sci. Total Environ.* **2011**, in press.
(31) Fei, H.; Leng, W.; Li, X.; Cheng, X.; Xu, Y.; Zhang, J.; Cao, C. Photocatalytic Oxidation of Arsenite over $TiO_2$: Is superoxide the main oxidant in normal air-saturated aqueous solutions? *Environ. Sci. Technol.* **2011**, *45*, 4532−4539.
(32) Martin, S. T.; Herrmann, H.; Choi, W.; Hoffmann, M. R. Time-resolved microwave conductivity (TRMC) 1. $TiO_2$ photoactivity and size quantization. *J. Chem. Soc. Faraday Trans.* **1994**, *90*, 3315−3322.
(33) Wardman, P. J. Reduction potentials of one-electron couples involving free radicals in aqueous solution. *Phys. Chem. Ref. Data* **1989**, *18*, 1637−1755.
(34) Kläning, U. K.; Bielski, B. H. J.; Sehesteds, K. Arsenic(IV). Pulse-radiolysis study. *Inorg. Chem.* **1989**, *28*, 2717−2724.
(35) Lenoble, V.; Deluchat, V.; Serpaud, B.; Bollinger, J.-C. Arsenite oxidation and arsenate determination by the molybdene blue method. *Talanta* **2003**, *61*, 267−276.
(36) Rasmussen, L.; Jebjerg Andersen, K. *Environmental health and human exposure assessment*, Chapter 2, World Health Organization in https://docs.google.com/viewer?url=http%3A%2F%2Fwww.who.int%2Fentity%2Fwater_sanitation_health%2Fdwq%2Farsenicun2.pdf (accessed October 26, 2010).
(37) Gutzeit, H. *Pharm. Ztg.* **1891**, *36*, 748−756.
(38) *Standard Methods for the Examination of Water and Wastewater*, 14th ed.; Rand, M. C., Greenberg, A. E., Taras, M. J., Eds.; American Public Health Association, American Water Works Association, Water Pollution Control Federation (APHA-AWWA-WPCF): Washington D.C., 1976; pp 284−286.
(39) *Standard Methods for the Examination of Water and Wastewater*, 14th ed.; Rand, M. C., Greenberg, A. E., Taras, M. J., Eds.; American Public Health Association, American Water Works Association, Water Pollution Control Federation (APHA-AWWA-WPCF): Washington D.C., 1976; pp. 283−284.
(40) Wagner, C. D.; Riggs, W. M., Davis, L. E., Moulder, J. F.; Mullenberg, G. E. *Handbook of X-Ray Photoelectron Spectroscopy*; Perkin Elmer Corporation: Eden Prairie, MN, 1978.
(41) Santhanam, K. S. V.; Sundaresan, N. S. Arsenic. In *Standard Potentials in Aqueous Solutions*; Bard, A. J., Parsons, R., Eds.; Marcel Dekker: New York, 1985; pp 162−172.
(42) Wilke, M.; Farges, F.; Petit, P.-E.; Brown, G. E. Jr.; Martin, F. Oxidation state and coordination of Fe in minerals: An Fe K-XANES spectroscopic study. *Am. Mineral.* **2001**, *86*, 714−730.
(43) Lamberti, C.; Bordiga, S.; Bonino, F.; Prestipino, C.; Berlier, G.; Capello, L.; D'Acapito, F.; Llabrés i Xamena, F. X.; Zecchina, A. Determination of the oxidation and coordination state of copper on different Cu-based catalysts by XANES spectroscopy in situ or in operando conditions. *Phys. Chem. Chem. Phys.* **2003**, *5*, 4502−4509.
(44) Jegadeesan, G.; Al-Abed, S. R.; Sundaram, V.; Choi, H.; Scheckel, K. G.; Dionysiou, D. D. Arsenic sorption on $TiO_2$ nanoparticles: Size and crystallinity effects. *Water Res.* **2010**, *44*, 965−973.
(45) Bearden, J. A.; Burr, A. F. Reevaluation of X-ray atomic energy levels. *Rev. Mod. Phys.* **1967**, *39*, 25−142.
(46) Quinn, R.; Mebrahtu, T.; Dahl, T. A.; Lucrezi, F. A.; Toseland, B. A. The role of arsine in the deactivation of methanol synthesis catalysts. *Appl. Catal., A* **2004**, *264*, 103−109.
(47) James-Smith, J.; Cauzid, J.; Testemale, D.; Liu, W.; Hazeman, J.; Proux, O.; Etschmann, B.; Philippot, P.; Banks, D.; Williams, P.; Brugger, J. Arsenic speciation in fluid inclusions using micro-beam X-ray absorption spectroscopy. *Am. Mineral.* **2010**, *95*, 921−932.
(48) Wang, C.; Pagel, R.; Bahnemann, D. W.; Dohrmann, J. K. Quantum yield of formaldehyde formation in the presence of colloidal $TiO_2$-based photocatalysts: Effect of intermittent illumination, platinization, and deoxygenation. *J. Phys. Chem. B* **2004**, *108*, 14082−14092.

(49) Zepp, R. G.; Hoigné, J.; Bader, H. Nitrate-induced photooxidation of trace organic chemicals in water. *Environ. Sci. Technol.* **1987**, *21*, 443−450.
(50) Moser, J.; Punchihewa, S.; Infelta, P. P.; Gratzel, M. Surface complexation of colloidal semiconductors strongly enhances interfacial electron-transfer rates. *Langmuir* **1991**, *7*, 3012−3018.
(51) Daniels, M. The radiation chemistry of arsenite. Part II. Oxygen-free solution. *J. Phys. Chem.* **1962**, 1475−1477.
(52) Muller, J. C.; Ferradini, C.; Pucheault, J. Radiolyse à très haute intensité des solutions darsenite. *Radiochem. Radioanal. Letters* **1972**, *10*, 53−58.
(53) Bejan, D.; Bunce, N. J. Electrochemical reduction of As(III) and As(V) in acidic and basic solutions. *J. Appl. Electrochem.* **2003**, *33*, 483−489.
(54) Breitenkamp, M.; Henglein, A.; Lilie, J. Mechanism of the reduction of lead ions in aqueous solution (a pulse radiolysis study). *Ber. Bunsen-Ges.* **1976**, *80*, 973−979.
(55) Allred, A. L.; Hensley, A. L. Jr. Electronegativities of nitrogen, phosphorous, arsenic, antimony and bismuth. *J. Inorg. Nucl. Chem.* **1961**, *17*, 43−54.
(56) Arango, A. C.; Carter, S. A. Charge transfer in photovoltaics consisting of interpenetrating networks of conjugated polymer and $TiO_2$ particles. *Appl. Phys. Lett.* **1999**, *74*, 1698−1700.
(57) Imanishi, A.; Tsuji, E.; Nakato, Y. Dependence of the work function of $TiO_2$ (rutile) on crystal faces, studied by a scanning Auger microprobe. *J. Phys. Chem. C* **2007**, *111*, 2128−2132.
(58) Behar, D.; Rabani, J. Kinetics of hydrogen production upon reduction of aqueous $TiO_2$ nanoparticles catalyzed by $Pd^0$, $Pt^0$, or $Au^0$ coatings and an unusual hydrogen abstraction; steady state and pulse radiolysis study. *J. Phys. Chem. B* **2006**, *110*, 8750−8755.
(59) Fernandez-Vega, A.; Feliu, J. M.; Aldaz, A. Heterogeneous electrocatalysis on well-defined platinum surfaces modified by controlled amounts of irreversibly adsorbed adatoms. *J. Electroanal. Chem.* **1991**, *305*, 229−240.
(60) Laroff, G. P.; Fessenden, R. W. Equilibrium and kinetics of the acid dissociation of several hydroxyalkyl radicals. *J. Phys. Chem.* **1973**, *77*, 1283−1288.
(61) Simic, M.; Neta, P.; Hayon, E. Reactions of hydroxyl radicals with unsaturated aliphatic alcohols in aqueous solution. A spectroscopic and electron spin resonance radiolysis study. *J. Phys. Chem.* **1973**, *77*, 2662−2667.
(62) Quinn, R.; Dahl, T. A.; Diamond, B. W.; Toseland, B. A. Removal of arsine from synthesis gas using a copper on carbon adsorbent. *Ind. Eng. Chem. Res.* **2006**, *45*, 6272−6278.
(63) Seredych, M.; Mahle, J.; Peterson, G.; Bandosz, T. J. Interactions of arsine with nanoporous carbons: Role of heteroatoms in the oxidation process at ambient conditions. *J. Phys. Chem. C* **2010**, *114*, 6527−6533.